Structural Changes in Bacteriorhodopsin during the Photocycle Measured by Time-Resolved Polarized Fourier Transform Infrared Spectroscopy

Lóránd Kelemen and Pál Ormos
Institute of Biophysics, Biological Research Centre of the Hungarian Academy of Sciences, Szeged H-6701, Hungary

ABSTRACT The structural changes in bacteriorhodopsin during the photocycle are investigated. Time resolved polarized infrared spectroscopy in combination with photoselection is used to determine the orientation and motion of certain structural units of the molecule: Asp-85, Asp-96, Asp-115, the Schiff base, and several amide I vibrations. The results are compared with recently published x-ray diffraction data with atomic resolution about conformational motions during the photocycle. The orientation of the measured vibrations are also calculated from the structure data, and based on the comparison of the values from the two techniques new information is obtained: several amide I bands in the infrared spectrum are assigned, and we can also identify the position of the proton in the protonated Asp residues.

INTRODUCTION

The protein pigment complex bacteriorhodopsin (bR) is found in high protein content regions of the cell membrane of *Halobacterium salinarum*, called the purple membranes. The chromophore is retinal connected to the Lys-216 residue of the protein backbone through a protonated Schiff base. bR is a light energy transducer upon light absorption it pumps protons across the cell membrane. After the absorption of a photon by retinal a sequence of reactions takes place: the photocycle. The photocycle runs through several intermediates (designated K, L, M, N, O) that are well distinguished by their visible absorption spectra.

Conformational changes of the protein are generally regarded crucial for the proton pumping function of bR. The correlated motion of both the chromophore and the protein moiety form the basis of the active pumping, consequently, the characterization of the molecular motions is the key to understanding the energy conversion process. By correlating structural and functional data,several structural markers have been found to characterize conformational changes that seem to be crucial for pumping. However, an exact identification of key conformational transitions in the photocycle could not be achieved. A number of methods have been used to investigate the protein structural changes that accompany the photocycle. Recently several results have been published in which the structure of bR was determined with atomic resolution, including the structures of several intermediate states of the pumping cycle. The first markers of the crucial structural changes have been determined and characterized in fairly great detail by Fourier transform infrared (FTIR) spectroscopy. A next step in the understanding is the identification of these markers with the recently determined molecular structures.

To characterize the orientation of a structural element in bR two angles are needed. A practical procedure is offered in FTIR spectroscopy, if the sample is a hydrated film of purple membranes oriented on an infrared (IR) window surface. On such a sample the option is to measure the angle of the element's IR dipole moment relative to the purple membrane normal in one experiment and then the angle between the projection of the element's IR dipole moment and that of the retinal's optical transition moment onto the purple membrane plane in a separate one. The first measurement does not need polarized actinic light but needs polarized IR measuring beam and measurement of the sample in two different sample positions relative to the IR beam.

We note here that the retinal position has previously been determined by polarized spectroscopy both in the visible (Barabás et al., 1983; Heyn and Otto, 1992) and in the IR (Earnest et al., 1986). The visible experiments resulted in an angle of $\sim 67^{o}$ between the retinal transition dipole and the membrabe normal. This is in agreement with the IR experiment in which the direction of the IR dipole moment of the retinal's delocalized C═C stretch, which is expected to be parallel to the axis of the polyene chain, also makes an angle of 64 to 71^{o} with the normal of the PM plane in the bR state. The authors determined also the orientation of the dipole of the C═O stretch in the protonated Asp-85 side chain in the M state relative to the PM normal. The angle between the two directions turned out to be 43 ± 4^{o}. This value is contradicted by Hatanaka et al. (1997) and Nabedryk and Breton (1986) in both latter papers this angle was found to be $\sim 35^{o}$ (36^{o} and 35 ± 5^{o}, respectively). Nabedryk and Breton (1986) additionally made estimations about the tilt of the protein backbone between the bR and the M states and concluded that the overall orientational change of the α-helices is $\sim 2^{o}$. However, local conformational changes cannot be and were not excluded.

Received for publication 3 May 2001 and in final form 23 August 2001.

Address reprint requests to Institute of Biophysics, Biological Research Centre of the Hungarian Academy of Sciences, Szeged H-6701, Hungary. Tel.: 36-62-433465; Fax: 36-62-433133; E-mail: pali@everx.szbk.u-szeged.hu.

0006-3495/01/12/3577/13 $2.00

The angle Θ between the projection of a structural element's IR dipole moment and that of the retinal's optical transition moment onto the PM plane can be determined by photoselective excitation and polarized IR measurement of an oriented bR sample (Fahmy et al., 1989, 1991; using slightly different nomenclature). In the first work the authors showed that in the ground state the direction of the retinal's C═C IR dipole moment makes an angle to the PM normal identical to that found for the optical transition moment and additionally proved that the angle Θ for this dipole is also zero. This simply means that the direction of the IR and the optical dipole moments coincide in the ground state. The Schiff base as the primary proton donor plays a key role in the proton transfer function of the protein. Its orientation therefore is crucial for the understanding of the events inside bR. Fahmy et al. (1989) determined without detailed calculations that the dipole of the Schiff-base's C═N stretch is perpendicular to the PM normal and that its angle Θ is approximately zero in the ground state. Later the same authors determined the orientation of several amino acid side chains also relative to both the PM normal and the retinal's optical transition (Fahmy et al., 1991). In the L state both the Asp-96 and Asp-115 groups give a positive band in the COOH region of the IR spectrum. Detailed analysis of these difference bands led to the conclusion that these two groups do turn between the bR and L states. The movement of the dipole moments is larger in the direction of the PM normal (~25°) than parallel to its plane (4–11°). This result is important because in the L state the primary proton movement from the Schiff base to Asp-85 has not yet occurred, but apparently rearrangement of important side chains has already started at some level. The direction of Asp-85 in the M state was characterized in greater detail by Breton and Nabedryk (1989) who measured the angle Θ of its C═O stretch to be 45°. This value and the previously found 43° (Earnest et al., 1986) (35° by Hatanaka et al., 1997) gives an approximation to the direction of the dipole of this amino acid side chain in the M state.

The aim of the presented work was to obtain new structural data from FTIR measurements and compare these with recent x-ray diffraction information. We performed experiments to determine values of Θ for bands of the IR difference spectra of the M or N states. For this we carried out time-resolved low-temperature polarized FTIR measurements combined with photoselection on wild-type bR. Our first goal was to estimate a direction relative to the retinal by using the angle Θ for several structural elements of bR to which an IR difference band was previously assigned. Next, we tried to assign amide I bands to parts of the bR backbone by comparison of the angle Θ measured with values calculated using recently published x-ray diffraction structures. By this procedure the structural information obtained by the different experimental techniques is expected to be unified, and an approach is made toward a coherent picture of the structural changes during function.

METHODS AND MATERIALS

Purple membranes of wild-type bR used for the photoselection measurements were prepared from strain S9 of *Halobacterium salinarum* (Oesterhelt and Stoeckenius, 1974). For the dried-rehydrated film a bR suspension of OD = 8 was prepared in 100 μM Trizma solution. Fifty microliters of this suspension was spread over an 8-mm diameter area on a 2-mm-thick CaF_2 window. This drop of suspension was dried under a gentle N_2 stream blowing downwards from above the center of the droplet, perpendicularly to the plane of the CaF_2 window. This way the inner 5 mm of the sample dried with even optical density suitable for homogeneous excitation and IR measurements. The CaF_2 window was placed into a temperature-controlled sample holder with the bR film facing inside. Approximately 3 μl of water was additionally dropped into the sample holder to rehydrate the bR film. Another 2-mm-thick CaF_2 window was used to hermetically seal the sample holder. The IR absorption of the dry sample was 0.65 in the amide I region at 1657 cm^{-1}, whereas that of the rehydrated sample was 0.9. The 3500-cm^{-1} water absorption band was used to check the process of rehydration. After 2 days this band was ~1.4 times larger than the absorption at 1657 cm^{-1}. The sample was masked by a 4-mm diameter aperture at its central region to make sure that the IR monitoring light and the exciting light illuminate identical part of the sample. The sample was kept at −8°C (265 K) throughout the entire measurement, and at this temperature 50 s after the start of the photocycle only 0.5% of the original difference signal remained, i.e., the total recovery of the bR state took ~1 min.

To facilitate photoselection the sample had to consist of aligned PM fragments. This property of our sample was checked by the method introduced in Rothschild and Clark (1979): using horizontally polarized IR beam we measured the IR absorption of the sample with the bR film's plane perpendicular to the IR beam (A_0) and when it was rotated 45° around the vertical axis (A_{45}). We calculated a dichroic difference spectrum from the two resulted absorption spectra (A_0–A_{45}). This showed an intense negative peak at 1667 cm^{-1} (amide I), one at 3250 cm^{-1} (amide A), and a positive one at 1548 cm^{-1} (amide II) (Fig. 1). The dichroic difference spectra were very similar to the one published on sample of aligned PM by Rothschild and Clark (1979).

The flash from a frequency doubled YAG laser (SURELITE I, Continuum, Santa Clara, CA) (λ = 532 nm, duration = 5 ns) started the photocycle. To not excite any intermediate in the repetitive experiments the sample was flashed in every 60 s. For the photoselection the exciting light had to be linearly polarized. Although the light emitted by the laser is already polarized, we applied a VIS polarizer to improve the polarization characteristics of the exciting light. The original beam diameter of the laser (~4 mm) was expanded to ~1 cm at the sample to ensure that only a homogeneous intensity region of the laser spot hits the sample and also to reduce the laser intensity. The laser intensity was chosen so that the amplitude of the calculated difference spectra was only 11% of that measured at saturation. The actinic laser light hit the sample with an angle of ~8° relative to the sample normal and to the direction of the IR beam.

The FTIR measurements were carried out on a Bruker IFS66 instrument (Bruker Optik GmbH, Ettlingen, Germany) capable of measuring with 85-ms time resolution in rapid scan mode. The IR bandwidth was reduced to 800 to 1970 cm^{-1} partly by the absorption of the CaF_2 window and partly by a low wavelength pass optical filter (L.O.T.–Oriel GmbH, Langenberg, Germany) that also blocked the detector from the YAG laser light. The spectral resolution of the measurement was 4 cm^{-1}, this parameter together with the fastest mirror scanning allowed the above time resolution. The zero filling factor was 4, this resulted data points in every 0.63 cm^{-1}. The measuring IR light was focused perpendicularly at the sample onto a spot of ~4 mm diameter. The small axial difference between the actinic and the measuring light beam directions did not introduce noticeable error to the measurement.

The IR polarizer for the linear dichroic measurement was a golden wire grid polarizer on KRS-5 glass (International Crystal Labs, Garfield, NJ), and it was placed between the sample holder and the detector. It was rotated to parallel and perpendicular positions relative

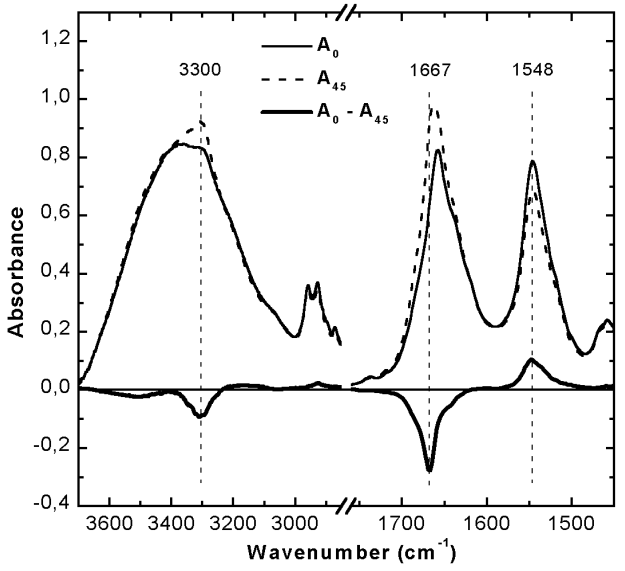

FIGURE 1 Absorption and dichroic spectra of rehydrated dried bR film measured in horizontally polarized IR light. The plane of the film is perpendicular to the optical axis of the IR beam (A_0) (*thin line*). The plane of the film is tilted 45° around the vertical axis, i.e., the normal of the film makes 45° with the optical axis of the IR beam (A_{45}) (*dashed line*). Dichroic spectrum (A_0–A_{45}) (*thick line*).

to the actinic laser light polarization by a small program embedded in the measuring OPUS software (Bruker Optik GmbH). One-hundred measurements with parallel and 100 measurements with perpendicular orientation were repeated 25 times, resulting in 2500 averages with both polarizer positions.

The raw results of the measurements were a series of single beam spectra, i.e., intensity spectra. The synchronization of the start of the measurement and the actinic laser flash was done such that the very first spectrum was measured just before the laser flash and stored as background ($SB(\lambda, t = 0)$), the others were measured after the flash ($SB(\lambda, t)$) in a predetermined sequence. Each spectrum in the time-resolved series needed a full scan of the interferometer, represented by its start-of-scan time and end-of-scan time. The time point corresponding to each spectrum was the average of these two characteristic times. The data acquisition was set up such that the spectra were averaged quasi-logarithmically to increase the S/N ratio: the first eight spectra were the result of single scans, every spectrum of the second eight was the average of two consecutive scans, every spectrum of the third eight was average of four consecutive scans, and so on. This way the final series contained 50 spectra spanning the 60-s measurement. The best time resolution was 85 ms at the beginning of the measurement, the worst was ~5.4 s at the end.

Data processing

Difference spectra were calculated from the measured single beam spectra as follows:

$$D(\lambda, t) = -\log \frac{SB(\lambda, t)}{SB(\lambda, t = 0)}$$

in which $D(\lambda, t)$ is the difference spectrum series consisting of 50 spectra, $SB(\lambda, t)$, and $SB(\lambda, t = 0)$ as described above. This calculation was performed on the data of both parallel and perpendicular polarization directions relative to the polarization of the actinic light resulting D_{II} and $D_{\perp}$, respectively. The difference spectra showed maximal amplitude at the first time-slice and gradually decayed to zero by the end of the 60-s-long measurement. We did not apply any noise reduction on the difference spectra before the additional calculations.

In previous papers (Breton and Nabedryk, 1989; Fahmy et al., 1991) the angle Θ was calculated using the amplitude of the IR bands taken directly from the difference spectra. This method cannot be applied for overlapping bands. To overcome this problem and to make this method usable for amide I difference bands, we first fitted sums of Gaussians to the difference spectra and then we used the time-dependent amplitudes of these Gaussian bands to determine Θ. We used global algorithm to fit the D_{II} and $D_{\perp}$ spectrum series together as one single series, i.e., the Gaussian band positions and half-widths constituted an identical set for all of the 2×50 spectra, and only the amplitude of each Gaussian band was allowed to change from spectrum to spectrum. The resulted series of Gaussian amplitudes were $A_{\text{II}}(t)$ and $A_{\perp}(t)$ for the two orientation directions consisting of 50-50 values each. The algorithm also added either a linear baseline (COOH region) or a constant baseline (amide I region) to the Gaussians. Because we dealt only with the changes of COOH groups and the protein backbone we performed the fitting only in limited regions: in regions 1712 to 1820 cm^{-1} and 1613 to 1704 cm^{-1}.

In addition, the time-dependent Gaussian amplitudes $A_{\text{II}}(t)$ and $A_{\perp}(t)$ were globally fitted with sums of three exponentials, which means that all of the Gaussian amplitudes had the same time constants (τ_1, τ_2, and τ_3) but different exponential amplitudes. Three exponentials were sufficient for the fitting because applying four exponentials always resulted in degenerated results.

The calculation of the angle Θ was carried out using the Gaussian amplitudes (Breton and Nabedryk, 1989):

$$\Theta(t) = \arccos\left(\left(\frac{A_{\parallel}(t) - A_{\perp}(t)}{A_{\parallel}(t) + A_{\perp}(t)} + 0.5\right)^{1/2}\right) \qquad (1)$$

This angle could be calculated for every IR band that can be fitted to a Gaussian. Because every band originates from the vibration of a dipole, this angle can be attributed to vibration modes and hence to structural elements. This way we determined the angle between the projection of the retinal and the projection of the particular structural element on the plane of the PM.

RESULTS AND DISCUSSION

We made polarized photoselection measurement on wild-type bR at T = −8°C (265 K) on rehydrated dried sample. The resulting D_{II} and $D_{\perp}$ difference spectra show very good signal-to-noise ratio: the noise ~1780 cm^{-1} where there is no difference signal was $\sim 10^{-6}$ OD, and the maximal signal at 1526 cm^{-1} was 2×10^{-3} OD (Fig. 2). However, ~1640 cm^{-1} where the water and the amide I absorption is high, there can be higher noise as well, but fortunately the signal is also large in that region. This S/N was sufficient for meaningful Gaussian fitting.

In Fahmy et al. (1991) the angle Θ is calculated using a factor c that enlarges dichroic difference A_{II}–$A_{\perp}$ to the value that would be found for complete photoreaction:

$$\tan^2 \Theta = \left(\frac{A_{\parallel}(t) + A_{\perp}(t) - c \times (A_{\parallel}(t) - A_{\perp}(t))}{A_{\parallel}(t) + A_{\perp}(t) + c \times (A_{\parallel}(t) - A_{\perp}(t))}\right) \qquad (2)$$

This correction was considered necessary for reasons such as light scattering in the sample and that in a realistic photoselection measurement the excitation may be higher than the optimal low intensity limit and the saturation effect

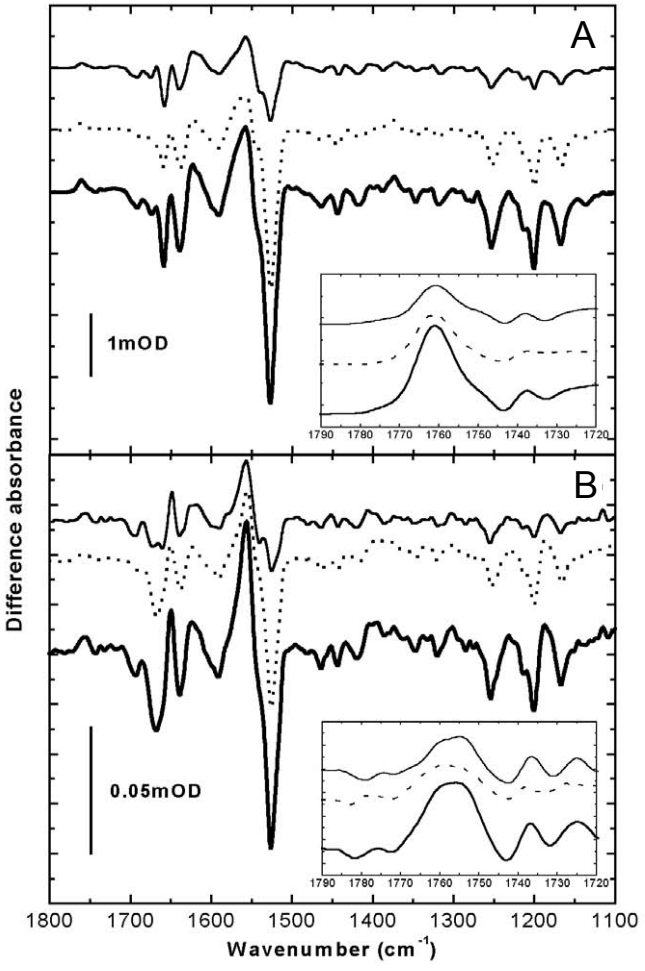

FIGURE 2 Difference spectra of rapid scan photoselection measurements (polarized actinic and measuring light) performed on rehydrated bR film ($T = -8$°C) 78 ms (*a*) and 30 s (*b*) after the photoexcitation. The polarization of the actinic and the measuring light were either parallel (D_{II}; *dashed line*) or perpendicular ($D_{\perp}$; *thin line*) to each other. The sum of the two orientations is represented by the (*thick line*) ($D_{II} + D_{\perp}$). Inserts, The expanded COOH region.

decreases the anisotropy. The authors showed that for the 1527 cm^{-1} C═C retinal band (Fahmy et al., 1989) Θ is zero, and they used its dichroic ratio to calculate the value of *c*, which was found to be 7 to 10. Using the same calculation we determined *c* for our measurement based on the intensity of the 1527 cm^{-1} band, and it turned out to be 2. This means that in our case the simpler Eq. 1 is valid, no additional correction is necessary.

COOH region

To determine the Gaussian amplitudes of the IR bands in the carboxyl vibration region we fitted the spectrum series with sums of Gaussians plus a linear baseline from 1712 cm^{-1} to 1820 cm^{-1} (Fig. 3, *a* and *b*). The linear baseline was needed because of the presence of the water continuum band in this region (Rammelsberg et al., 1998). The intensities of the COOH bands are small as compared with the rest of the spectrum, and at the later time slices of the spectra series the fit was uncertain. For this reason the region was fitted only for spectra taken in the 0 to 20-s interval.

The obtained bands well correspond to the band positions observed in the M and N intermediates: the 1761 cm^{-1} and 1738 cm^{-1} positive bands are typical for the M, whereas the 1756 cm^{-1} positive and 1743 cm^{-1} negative bands are typical for the N state (Ormos et al., 1992; Sasaki et al., 1994; Yamazaki et al., 1998) (Table 1). We also obtained another positive band at 1725 cm^{-1} with intensity similar to that of the 1738 cm^{-1} band. It can also be observed in the M spectrum of the polarized measurement in Nabedryk and Breton (1986). The origin of this band is not clear at the moment, but one possibility is the special alignment characteristics of the sample. However, this band was too wide and its time-dependent intensity was too noisy, giving unreliable Θ value.

The time-dependent Gaussian amplitudes of the COOH bands (both A_{II} and $A_{\perp}$) could be fitted to a sum of three exponentials (Fig. 3, *c* and *d*). The obtained τ values were: 0.33 s, 2.53 s, and 11.66 s. Table 1 depicts the exponential amplitudes for the COOH bands. The fact that the exponential fitting gave three macroscopic rate constants shows that there are three intermediate forms involved (Nagle, 1991). Because the very first difference spectrum at $t = 78$ ms is that of an almost pure M, only the presence of forms after the M intermediate is possible. In addition, from the kinetic analysis of Váró and Lányi (1991), it follows that the early M is not present anymore at this time. We know that at low temperatures the O form is not present either (Ludmann et al., 1998; Váró and Lányi, 1991), therefore the measured difference spectra are mixtures of the M and N forms. In this work we do not attempt to perform a detailed kinetic analysis, but assume that some of the three exponential components describe M→N transition and some of them N→bR decay. This is supported by that in the case of the negative 1743 cm^{-1} and the positive 1756 cm^{-1} bands, both typical for the N state, the sign of the first exponential amplitude (a_1) is different form the last two (a_2, a_3), meaning that the a_1 represents an M→N transition, whereas the a_2 and a_3 belong to decays. The exponential amplitudes of the 1761 cm^{-1} band all have positive sign, showing its decay throughout the whole process. The opposite sign and large absolute value of a_1 relative to a_2 and a_3 in the case of the 1756 cm^{-1} band indicate that this band is still building up during at least the first 500 ms of the measurement. Because this band is characteristic to the N state, we can conclude that by ~1 s large population of the bR transformed from M to N. The a_3 amplitude of this band and that of the 1743 cm^{-1} band are the largest in both cases, which shows that this exponential amplitude most likely represents the N→bR decay.

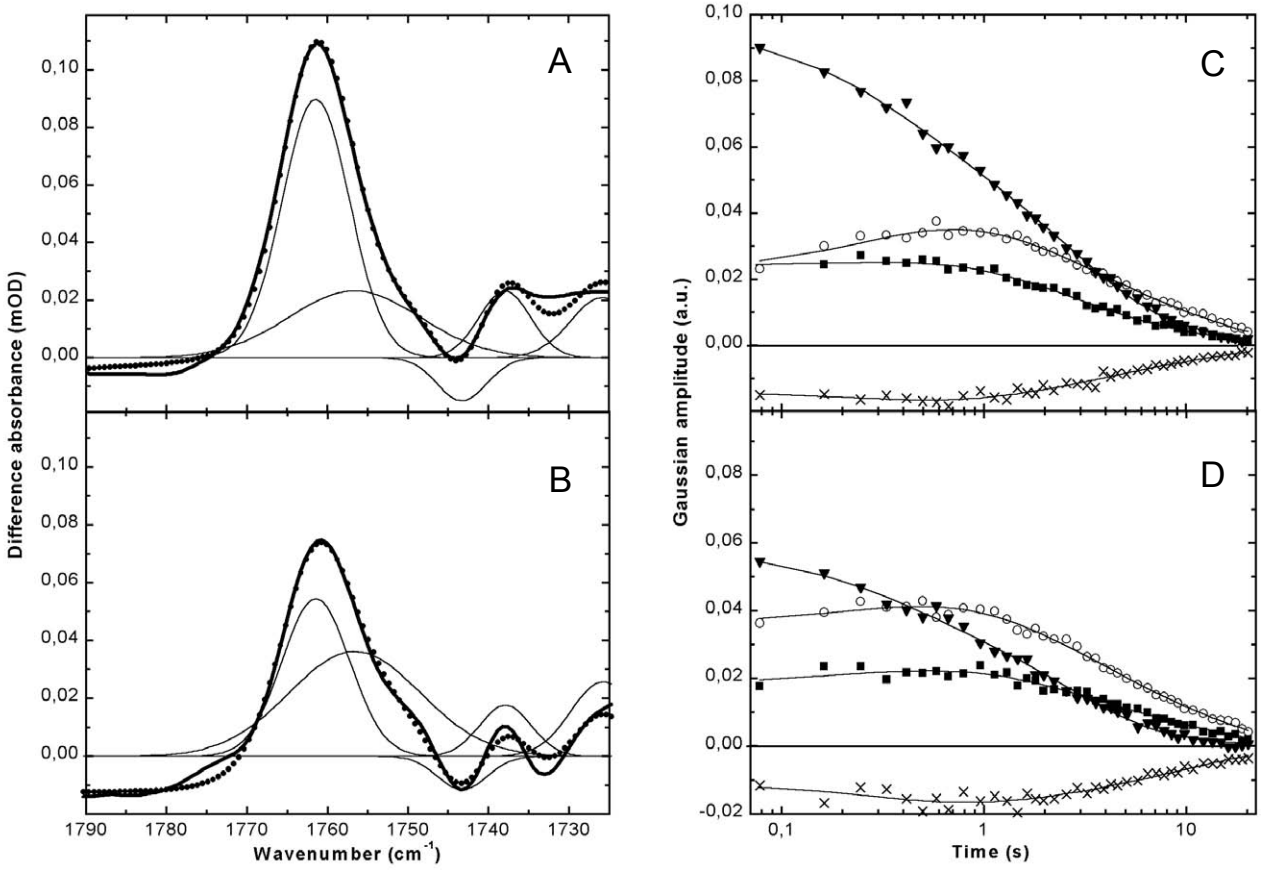

FIGURE 3 Gaussian fit to the 1712 cm^{-1} to 1820 cm^{-1} region of the photoselection difference spectra measured on rehydrated bR film ($T = -8$°C). Figures on the left (parallel polarization (*a*) and perpendicular polarization (*b*)) show the original difference spectra 78 ms after photoexcitation (*thick line*), the fitted curves to these early spectra (*dotted line*), and the individual Gaussian components (*thin line*). Figures on the right (parallel polarization (*c*) and perpendicular polarization (*d*)) show the time evolution of the Gaussian amplitudes of the 1738 cm^{-1} (■), the 1743 cm^{-1} (×), the 1756 cm^{-1} (○), and the 1761 cm^{-1} (▼) bands together with the exponential fit to these time dependent amplitudes (*thin line*).

In Table 1 there are two Θ values indicated for each band. The first one always corresponds to Θ at $t = 78$ ms, the last one to Θ at $t = 20$ s after the start of the photocycle, except the 1761 cm^{-1} band, where the last one corresponds to 8 s. This is because the Gaussian amplitudes A_{II} and $A_{\perp}$ of the 1761 cm^{-1} band become too small after 8 s so the ratio in Eq. 1 gives large noise.

The Θ angle values calculated from the Gaussian fitting change slightly with time (Fig. 4). This may come either from uncertainties of the fitting, because of the relatively small signal in this region, or from the fact that the orientation of the COOH groups change in time indeed. The first explanation is more likely because such a continuous change in side-chain orientation would result in change of

TABLE 1 Result of the Gaussian fit to the difference spectra in the COOH region

Band position	1761 cm^{-1}	1756 cm^{-1}	1743 cm^{-1}	1738 cm^{-1}
Sign of the band	Positive	Positive	Negative	Positive
Θ Value	30–25°	55–47°	40–55°	40–53°
Exponential amplitudes for $A_{\parallel}$ spectra ($a_{i,\parallel}$), $i = 1, 2, 3$	$a_1 = 0.279$ $a_2 = 0.582$ $a_3 = 0.116$	$a_1 = -0.226$ $a_2 = 0.208$ $a_3 = 0.235$	$a_1 = 0.062$ $a_2 = -0.088$ $a_3 = -0.111$	$a_1 = -0.069$ $a_2 = 0.213$ $a_3 = 0.094$
Exponential amplitudes for $A_{\perp}$ spectra ($a_{i,\perp}$), $i = 1, 2, 3$	$a_1 = 0.161$ $a_2 = 0.385$ $a_3 = 0.044$	$a_1 = -0.142$ $a_2 = 0.232$ $a_3 = 0.264$	$a_1 = 0.091$ $a_2 = -0.037$ $a_3 = -0.158$	$a_1 = -0.091$ $a_2 = 0.128$ $a_3 = 0.144$
Assigned to	Asp-85 in M	Asp-85 in N	Asp-96 in N	Asp-115 in M, N

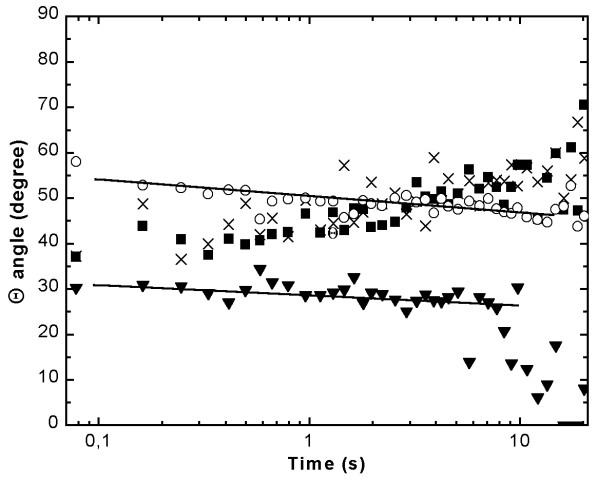

FIGURE 4 The time dependence of the angle Θ between the projection of the retinal's IR dipole moment to the membrane plane and that of the IR dipole moments of COOH groups responsible for the individual bR difference bands: 1738 cm^{-1} (■), 1743 cm^{-1} (×), 1756 cm^{-1} (○), and 1761 cm^{-1} (▼). The continuous lines are inserted only to guide the eye.

the environment of the group, and this latter would give rise to a continuous frequency shift, too. This kind of band shift was not observed in our data. The time independence of the angle Θ generalizes earlier results of Czégé et al. (1982), who found that the anisotropy factor of ultraviolet chromophores, i.e., tryptophan does not change while they are in a perturbed state. These results indicate that the protein parts observed have constant orientation during the lifetime of a particular intermediate, i.e., all conformational changes are synchronized to the well-known transitions in the photocycle.

We know from the literature that both the 1761 cm^{-1} and the 1756 cm^{-1} bands originate from the C═O stretching vibration of the protonated Asp-85 group: the first band is present in the M state, the latter one is in the N state (Kandori, 1998; Sasaki et al., 1994; Ormos et al., 1992). The difference in the frequency is due to the different environment of the group in the two intermediates. The nature of this environmental change between M and N has not been yet clarified, in other words it has not been answered whether the environmental change is connected to the movement of this group (when the direction of the C═O dipole does change), or it happens without any movement (for example a formation of a new H bond to the Asp-85 and the orientation of the dipole remains the same) (Heberle, 2000; Sasaki et al., 1994). There is only one hint for the position of the Asp-85 in the literature: in Kandori (1998) it is stated that there is no significant change in its position between M and N. We note that this statement is based only on the measurement of the angle between the dipole moment and the normal of the PM plane, and therefore it is necessarily an underassumption.

Our measurement is, however, a direct proof that this group does change its orientation during the M→N transition. For the 1761 cm^{-1} band that is the frequency of the Asp-85 in the M state we measured $\Theta < 30^{o}$ and for the 1756 cm^{-1}, which is its frequency in the N state we obtained $45 < \Theta < 55^{o}$ during the whole process. This means that the projection of the vibration mode of the group's C═O stretching onto the membrane plane clearly changes its orientation during M→N by ~20°. Because this value refers only to the projection of the movement, the absolute rotation can be even larger.

The directions of the CO bonds of the Asp-85, Asp-96, and Asp-115 carboxyl groups were calculated using recent x-ray structural models of the bR, M, and M_N intermediates. The bond directions can also be determined from the FTIR difference spectra. In control normal mode calculation on formic acid as a model for the protonated carboxyl group we determined that the direction of the vibrational dipole moment of the C═O stretching mode deviates less than 4° from the direction of the C═O bond, which is less than the error of our measurement. Based on these two calculations a comparison was made between the Θ angle values measured by FTIR (Table 1) and the directions of the CO bonds obtained from the x-ray structures (Table 2). The two angle values in each row of Table 2 refer to the directions of the two CO bonds in the carboxyl groups.

In the case of Asp-85 for both chosen M-state structures the calculated CO angles (48 and 51°) of the first O atom

TABLE 2 Directions of CO bonds of carboxyl groups in ground state (bR) and in M or M_N state calculated from x-ray structures of wild-type (WT) and mutant bacteriorhodopsin

		WT bR	WT bR	WT M	E204Q bR	E204Q M	D96N M_N
Asp-85 (M)	1st O			48°		51°	
	2nd O			86.5°		82°	
Asp-85 (N)	1st O						82.5°
	2nd O						68°
Asp-96	1st O	58°	65°		64°		
	2nd O	36°	38.5°		36.5°		
Asp-115	1st O			45°		38.5°	43.5°
	2nd O			84°		84°	64.5°
References		Belrhali et al., 1999	Sass et al., 2000	Sass et al., 2000	Luecke et al., 2000	Luecke et al., 2000	Luecke et al., 1999

agree fairly well with the Θ angle measured for the protonated group in the M state (1761 cm^{-1} band, 25–30°). (The agreement is even better if we consider that in the structure of Sass et al. (2000) the measured structure is assumed to be a mixture of M and N, and the Θ value for the 1756 cm^{-1} N band is 47–55°.) This oxygen is the one pointing away from the retinal, which indicates that this forms the C═O bond, and the other O atom pointing toward the Schiff base participates in the C—O bond, bearing the accepted H. This supports the general notion that the O atom, which in the ground state is H bonded to the water molecule localized between the Schiff base and Asp-85 gets protonated in M.

Note that by identifying the C═O bond, this method is capable of determining which oxygen is protonated in a carboxyl group. The same procedure can be applied to the other aspartic residues, too.

The negative 1743 cm^{-1} band, which shows the deprotonation of the Asp-96 group (Gerwert et al., 1990), is still growing at the beginning of the measurement and has negative a_1 and positive a_2 and a_3 exponential amplitudes, which corresponds to the fact that this band is present in the N state. From this negative band it follows that the projection of the IR transition dipole of the C═O stretch of the Asp-96 group in the ground state makes an 47 ± 7° angle with that of the retinal (Table 1). The angles calculated for the second CO bond of Asp-96 are reasonably close to this range for all three x-ray models (Table 2). This agreement is better than for Asp-85 and indicates that the unprotonated O atom of Asp-96 in the ground state is pointing to the center of the molecule, and the one pointing to the cytoplasmic side will subsequently donate its proton to the Schiff base.

The 1738 cm^{-1} positive band is the result of the environmental change of the protonated Asp-115 residue that evolves during the M state and remains present throughout the N state (Sasaki et al., 1994). Its measured Θ value matches the first CO bond's angle value for all three x-ray structures. This C═O bond in the ground state consequently points toward the extracellular surface.

Amide I region

Twelve bands were needed for the fitting of the amide I region of the difference spectra between 1613 cm^{-1} and 1704 cm^{-1} with sums of Gaussians and a constant baseline. There were bands that resulted in negligible Gaussian amplitude either in the A_{II} or in the $A_{\perp}$ spectrum, but which were necessary to fit the two types of spectra together. Whereas these bands could not be used for Θ angle calculation, the rest of the bands that are characteristic for the difference spectrum of the M or the N state (Ormos, 1991; Ormos et al., 1992; Rothschild et al., 1993; Yamazaki et al., 1998) could be fitted precisely and gave reliable Gaussian amplitudes and Θ values. The maximal residuum of the fit was smaller than 5% of the signal.

The characteristic main bands were fitted to the following positions: 1624 cm^{-1} ⊕, 1639 cm^{-1} ⊖, 1652 cm^{-1} ⊕, 1657 cm^{-1} ⊖, 1667 cm^{-1} ⊖, 1674 cm^{-1} ⊖, 1692 cm^{-1} ⊖, and 1699 cm^{-1} ⊖ (Fig. 5, *a* and *b*) (⊕, positive band; ⊖, negative band). The first two bands in this list are the combination vibration of the C═N bond of the Schiff base. The 1624 cm^{-1} band represents its frequency in the M and with a smaller intensity in the N state and comes from the vibration of the 13 *cis* retinal. The 1639 cm^{-1} is a frequency characteristic for the bR state (Bagley et al., 1982; Smith et al., 1985; Earnest et al., 1986) and comes from the all-*trans* retinal. The rest of the bands have previously been attributed to the vibration of the protein's backbone.

The low noise content of the measurement in the amide I region resulted in very noiseless kinetics to the Gaussian amplitudes, so the deviation of the calculated Θ(*t*) values are small too (Fig. 6). The time dependence of the Θ angles (apart from the random noise) is negligible for five of these bands except for the 1652 cm^{-1} and the 1699 cm^{-1} bands. This means that the Θ value for the five bands does not change in time. The time dependence of the Θ angle in the case of the 1652 cm^{-1} and the 1699 cm^{-1} bands can be described only as a trend: the first one decreases, the second one increases, but here the increase is greatly masked by noise. There is another difference band, however, which is characteristic for the N state: the 1667 cm^{-1} band. The Gaussian amplitudes obtained from fitting this band show such time dependence that the calculation of the Θ angle is not straightforward. The behavior of these amplitudes is discussed later.

The time dependence of the Gaussian amplitude series ($A_{II}(t)$ and $A_{\perp}(t)$) in this case also was explored by fitting them to a sum of exponentials (Fig. 5, *c* and *d*). The obtained τ values were: 0.44, 2.43, and 11.74 s, which correspond well to those fitted to the time-dependent Gaussian amplitudes of the COOH bands. Table 3 shows the calculated Θ values and exponential amplitudes for the amide I bands. In the row "type" the letter "M" indicates bands that are present in the difference spectrum of the M state and are insignificant in that of the N state according to the literature, and the letter "N" indicates the ones that are present either exclusively in the spectrum of N or both in that of N and M.

Retinal Schiff base

From Table 3 it is clear that the retinal's Schiff base changes its position at one time between the bR and the M states indicated by the change of the Θ angle of the dipole moment from ~15 to ~58°. The appearance of the SB bands cannot be determined in terms of intermediate states with the present time resolution measurement. The band pair is very likely present already in the K state (Bagley et al., 1982; Weidlich and Siebert, 1993), but it surely is in the L state (Ormos et al., 1992). From this we can conclude that the two

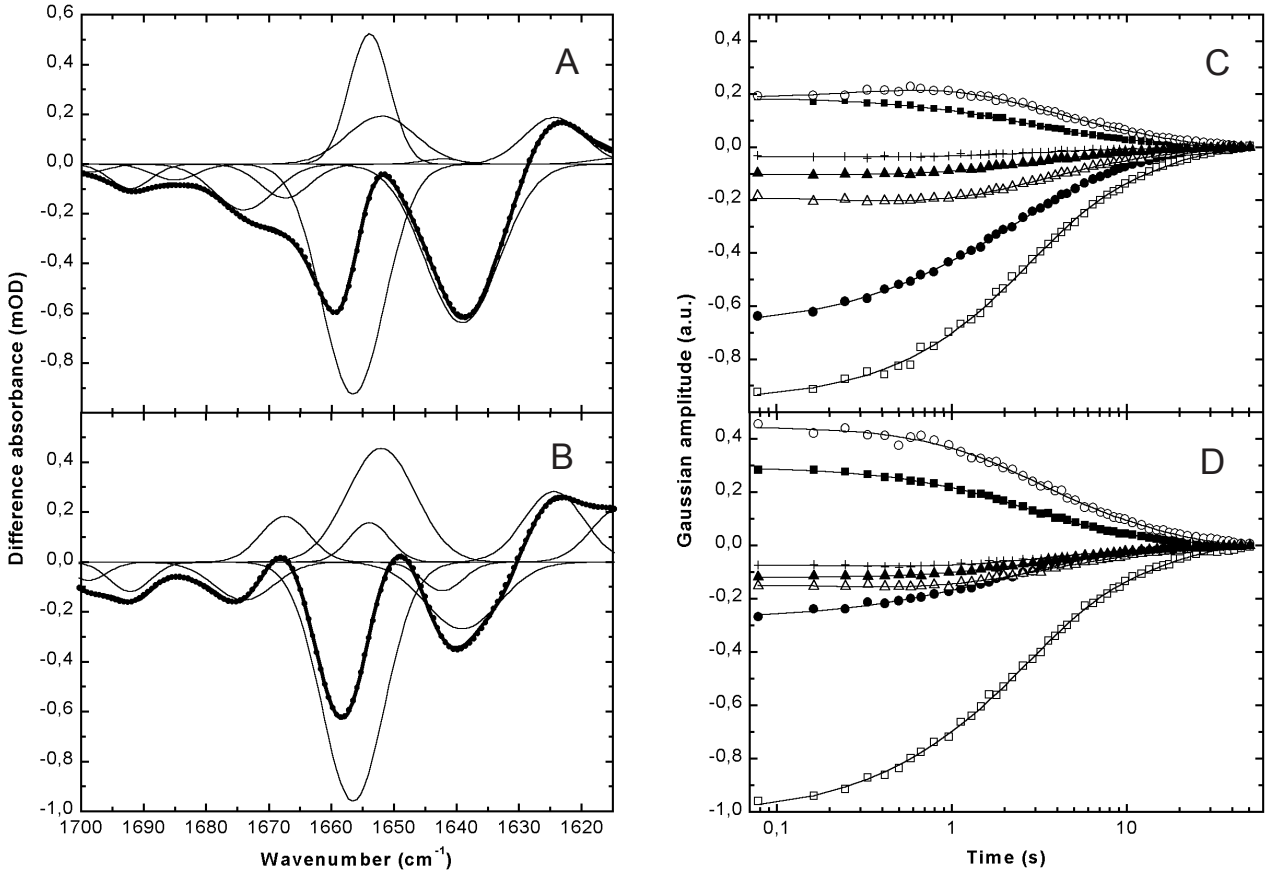

FIGURE 5 Gaussian fit to the 1613 cm^{-1} to 1704 cm^{-1} amide I region of the photoselection difference spectra measured on bR film (t = −8°C). Figures on the left (parallel polarization (*a*) and perpendicular polarization (*b*)) show the original, unsmoothed spectra 78 ms after photoexcitation (*thick line*), the fitted curve to these early spectra (*dotted line*), and the individual Gaussian components (*thin line*). Figures on the right (parallel polarization (*c*) and perpendicular polarization (*d*)) show the time evolution of the Gaussian amplitudes of the 1624 cm^{-1} (■), the 1639 cm^{-1} (●), the 1652 cm^{-1} (○), the 1657 cm^{-1} (□), the 1674 cm^{-1} (△), the 1692 cm^{-1} (▲), and the 1699 cm^{-1} (+) bands together with the exponential fit of these time dependent amplitudes (*thin line*).

bands are created not because of the deprotonation of the SB (because it deprotonates only in M) but because of the isomerization. To determine the value of Θ of the SB in an earlier protonated but already isomerized state, one needs to measure similar photoselection measurements on the K and/or L states. It is still a question of how the deprotonation (i.e., M accumulation) affects this angle. Here we can claim that in the all-*trans* protonated bR state the direction of the projection of the C═N bond's dipole makes a 15 ± 3° angle with that of the optical transition moment, and in the deprotonated 13-*cis* M state this angle is already 58 ± 2°. The two SB bands clearly belong to the "M" type according to their kinetics, in clear correspondence with papers showing that in the N spectrum these bands either are not present anymore or only with very small intensity (Pfefferlé et al., 1991; Ormos et al., 1992; Sasaki et al., 1992, 1994; Yamazaki et al., 1998).

Amide I band assignment

The rest of the bands in the amide I region originate from the C═O stretch mode of the peptide bond in the protein backbone. It has been known that these bands represent large-scale conformational changes in the protein structure. However, their assignment has not been done so far. With the results of our Θ angle measurements and by comparing them with recently published x-ray structural data (Belrhali et al., 1999 (PDB file, 1QHJ); Luecke et al., 1999 (PDB files, 1C8R and 1C8S); Luecke et al., 2000 (PDB file, 1F50); Sass et al., 2000 (PDB file, 1CWQ)), the chain segments that are responsible for these protein backbone difference bands and therefore are involved in the large-scale conformational changes in bR can be identified.

The area of the Gaussian curves corresponding to each amide I band can be used to estimate the number of groups that can be the origin of the particular IR difference band. This can be done by comparing the area of the amide I band

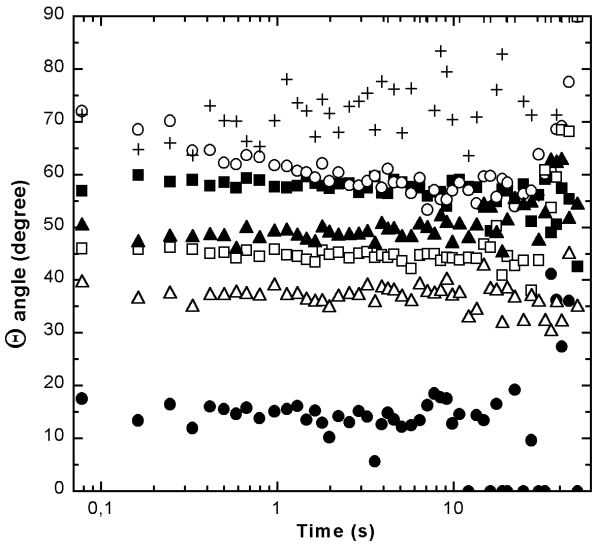

FIGURE 6 The time dependence of the angle Θ between the projection of the retinal's IR dipole moment and that of the IR dipole moments of C═O peptide groups responsible for the amide I difference bands: 1652 cm^{-1} (○), 1657 cm^{-1} (□), 1674 cm^{-1} (△), 1692 cm^{-1} (▲), and 1699 cm^{-1} (+). The Θ of the two Schiff-base bands are also shown: 1624 cm^{-1} (■) and 1639 cm^{-1} (●).

of the bR absolute absorption spectrum and the area of the chosen Gaussian. The process described below needed a separate unpolarized measurement on the same sample at the same temperature. First we assume that at saturating laser intensity at most 33% of the bR molecules is converted to M (Becher and Ebrey, 1977; Goldschmidt et al., 1977). In this experiment we used an excitation level to achieve 81% of saturation, i.e., 27% of bR was photoconverted. It was determined that the first difference spectrum taken at $t = 78$ ms contained ~90% of the M state's spectrum therefore ~24% of bR is in the M state at this time. In this spectrum the area of the Gaussian fitted to the 1657 cm^{-1} amide I band was 0.0546. The area of the entire amide I band in the absolute absorption spectrum was 32.36, this is produced by the stretching vibration of the C═O peptide bond of the 248 residues. The share of the 24% photoconverted bR molecules from the area of the total absorption band is 7.76. We also have to consider that the direction of the transition moments of the C═O bond makes an average of 35° angle with the axis of the α-helices (Marsh et al., 2000), which in our case is roughly the normal of the sample. From these data we calculated that ~5.25 amino groups are needed to produce the 1657 cm^{-1} difference band. The rest of the amide I difference bands are much smaller, so they very likely originate from single amino acids. In the case of the bands that correspond to single amino acid side chains, there is hope to identify the corresponding groups. Note that this also means an inherent limitation of the method: in cases of highly overlapping bands, assignment is not possible. Consequently, potentially "interesting" side chains may be not identified. It has to be pointed out here, too, that unambiguous assignment can be done by labeling specific groups, so the assignments done without this (like here) have to be regarded as tentative.

The existence of good quality x-ray structure of wild-type and mutant bR and the measured Θ angles form the kinetically analyzed bands made the assignment of the protein backbone bands possible. To get a more precise picture, the comparison of four ground state and two M form x-ray structures were performed in terms of the direction of the peptide C═O dipole and were used in addition for the assignment. For the assignment we used the amide band intensities together with the PDB files with the accession codes 1CWQ, 1QHJ, 1C8R, 1C8S, and 1F50. Because there are different numbers of amino acid groups in these structural models, there are regions that cannot be compared. The assignment procedure was performed as follows: as a first step of the procedure we determined the orientation of the IR transition dipole moment of the C═O stretching vibration of each peptide bond in the coordinate system of the actual x-ray structure resulting in the $M_{IR,C=O}$ vectors. In doing this, two assumptions were made: 1) the dipole moment vector is in the peptide plane and 2) the dipole moment vector makes an angle of $\delta_M = 20°$ with the direction of the C═O bond, pointing away from the N atom of the peptide bond (Marsh et al., 2000; Rothschild and Clark, 1979). The second step was to calculate the Θ angle for each dipole moment: we projected the IR dipole moment vectors

TABLE 3 Result of the Gaussian fit to the difference spectra in the amide I region

Band position	1624 cm^{-1}	1639 cm^{-1}	1652 cm^{-1}	1657 cm^{-1}	1674 cm^{-1}	1692 cm^{-1}	1699 cm^{-1}
Sign of the band	Positive	Negative	Positive	Negative	Negative	Negative	Negative
Θ Value	58 ± 2°	15 ± 3°	70–55°	45.5 ± 1.5°	37 ± 2°	49 ± 2°	65–80°
Exponential amplitudes for $A_{\parallel}$ spectra, $(a_{i,\parallel})$ $i = 1, 2, 3$	$a_1 = 0.006$ $a_2 = 0.119$ $a_3 = 0.063$	$a_1 = -0.102$ $a_2 = -0.415$ $a_3 = -0.157$	$a_1 = -0.096$ $a_2 = 0.135$ $a_3 = 0.142$	$a_1 = -0.016$ $a_2 = -0.646$ $a_3 = -0.296$	$a_1 = 0.069$ $a_2 = -0.142$ $a_3 = -0.113$	$a_1 = 0.017$ $a_2 = -0.077$ $a_3 = -0.044$	$a_1 = 0.009$ $a_2 = -0.029$ $a_3 = -0.015$
Exponential amplitudes for $A_{\perp}$ spectra, $(a_{i,\perp})$ $i = 1, 2, 3$	$a_1 = 0.005$ $a_2 = 0.197$ $a_3 = 0.094$	$a_1 = -0.051$ $a_2 = -0.164$ $a_3 = -0.059$	$a_1 = -0.024$ $a_2 = 0.262$ $a_3 = 0.212$	$a_1 = -0.076$ $a_2 = -0.639$ $a_3 = -0.291$	$a_1 = 0.044$ $a_2 = -0.102$ $a_3 = -0.088$	$a_1 = 0.015$ $a_2 = -0.080$ $a_3 = -0.053$	$a_1 = 0.025$ $a_2 = -0.052$ $a_3 = -0.045$
Type	M	M	N	M	N	N	N

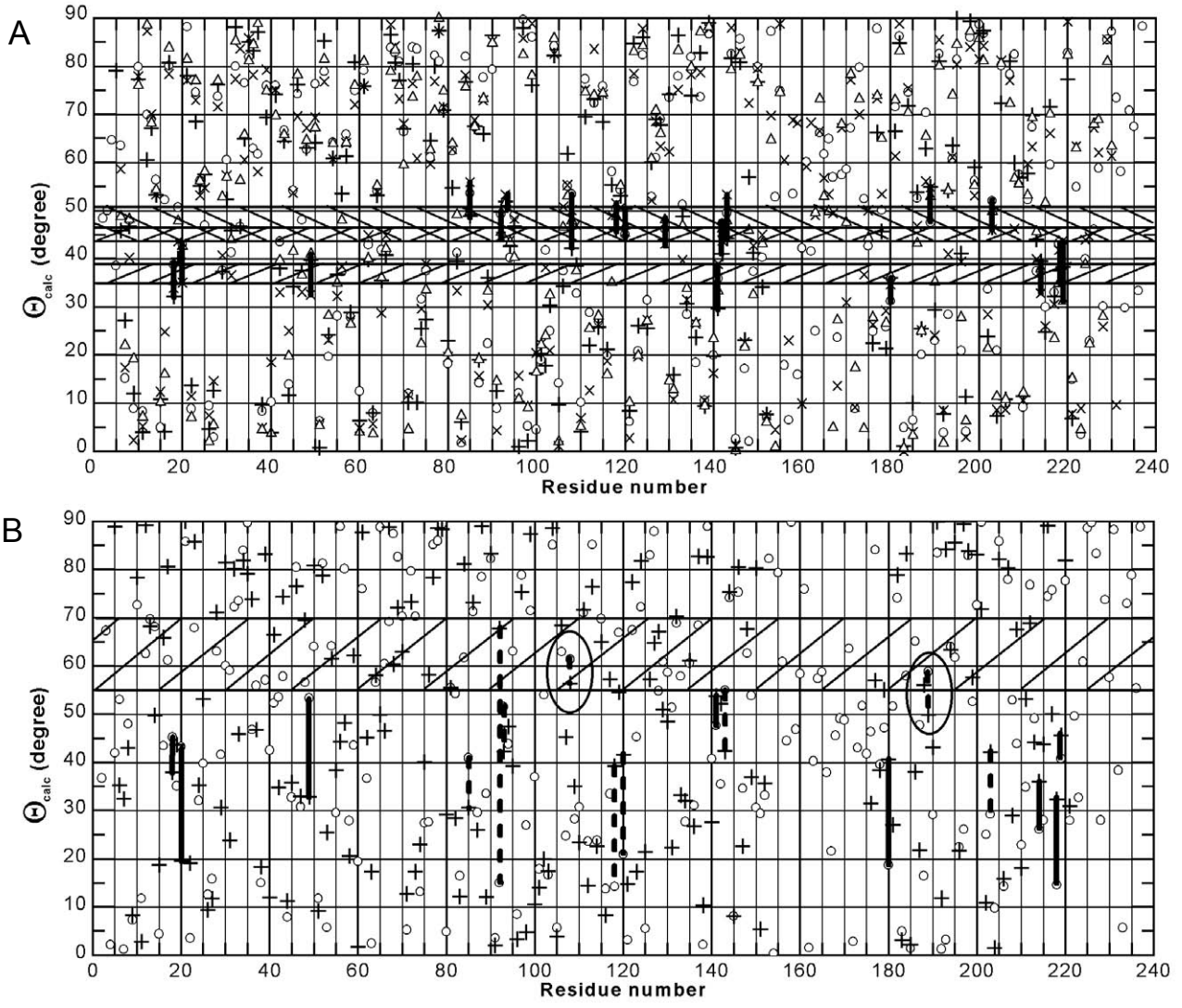

FIGURE 7 Calculated Θ_{calc} angles of the C═O peptide groups of each residue in the bR molecule in the ground state (*a*) and in the M state (*b*). Subfigure (*a*) contains angle values from four x-ray structures: ○, wild type from Sass et al. (2000); ×, wild type from Belrhali et al. (1999); +, mutant D96N from Luecke et al. (1999); and △, mutant E204Q from Luecke et al. (2000). We defined the angular regions for the amide I bands by the photoselcetion measurement: 1657 cm^{-1} band (*shaded* ××××), 1674 cm^{-1} band (shaded /), and 1692 cm^{-1} band (shaded \). The vertical bars span over the four Θ_{calc} values of the amino acid side chains that match one assignment criterium. In subfigure (*b*) only two structures are presented: ○, Sass et al. (2000); +, Luecke et al. (1999). The vertical bars cover the two Θ_{calc} values calculated for the amino acid side chains assigned to the 1674 cm^{-1} (*solid lines*) and the 1692 cm^{-1} (*dashed lines*) amide bands. Circled are the angle values of Ile-108 and Trp-189 in the M state.

($M_{IR,C═O}$) of every C═O bond and the electronic transition moment of the retinal ($M_{EL,RET}$) to the membrane plane (referred to as $m_{IR,C═O}$, and $m_{EL,RET}$, respectively), and calculated the angle between them (Θ_{calc}). We assumed that the direction of $M_{EL,RET}$ is parallel to the retinal's physical axis (Fahmy et al., 1989). Fig. 7 shows the obtained Θ_{calc} angles for the four ground state and two M state structures.

Finally, a selection was made among the amino acid side chains using the Θ_{calc} angles from the four ground state models and the measured Θ angles of the three amide I bands. The time-resolved measured Θ angle of each amide I band (1657 cm^{-1}, 1674 cm^{-1}, and 1692 cm^{-1}) has an average value in the 0 to 90° scale. When plotted against the residue serial number, the Θ_{calc} values obtained from the four models (Fig. 7) might match one of the measured Θ angles. The assignment is based on two reasonable matching criteria by which the residues are selected. First, a residue is selected if all four corresponding Θ_{calc} values from the x-ray structures are in the range defined by the minimum and the maximum of the measured Θ angle of an amide I band. Second, one is selected if two of its four Θ_{calc} values are closer to the average of the measured Θ than its deviation ($\pm 2°$) and the other two are closer than 7°. This selection resulted in five groups for the 1657 cm^{-1} band,

TABLE 4 Comparison of the orientation of the amide C=O bonds obtained from FTIR experiments with X-ray structure data

IR difference band	1657 cm^{-1}	1674 cm^{-1}	1692 cm^{-1}
Amino acid side chains associated to the difference band	Leu-92 (Θ = 44.5–49.7°) Gly-120 (Θ = 45–50.4°) Lys-129 (Θ = 43.1–48°) Thr-142 (Θ = 41–47.3°) Ile-203 (Θ = 46–52°)	Ala-18 (Θ = 32.1–38.8°) Met-20 (Θ = 35–43°) Val-49 (Θ = 32.5–40.9°) Ser-141 (Θ = 29.6–38.9°) Val-180 (Θ = 31.2–36.4°) Ser-214 (Θ = 32.8–39.5°) Gly-218 (Θ = 34.7–43.2°) Phe-219 (Θ = 31.1–43.9°)	Asp-85 (Θ = 48.9–56°) Leu-92 (Θ = 44.65–49.7°) Leu-93 (Θ = 51.6–53.3°) Ile-108 (Θ = 42.2–53.2°) Met-118 (Θ = 46–51.5°) Gly-120 (Θ = 45–50.4°) Ala-143 (Θ = 44.2–53.3°) Trp-189 (Θ = 47.5–54.9°) Ile-203 (Θ = 46–52°)

eight groups for the 1674 cm^{-1} band, and nine groups for the 1692 cm^{-1} band, which are represented by vertical bars in Fig. 7 *a*.

From the bands shown in Table 3 we could choose the 1657 cm^{-1}, 1674 cm^{-1}, and 1692 cm^{-1} bands to assign to the structure because the angular range of Θ of the other two amide bands were too wide, consequently the assignment procedure yielded too many amino acid groups as possible origin of these difference bands. The fact that these three bands are negative in the difference spectrum means that their frequency represents the bR ground state. This is why we chose amino acid groups from the ground state structure Θ_{calc} to match the bands' measured Θ angle. The result of the assignment procedure is shown in Table 4.

With the reasonable assumption that the protein structure of D96N by Luecke et al. (1999) and wild type by Sass et al. (2000) after the large conformational changes represents both late M and N like structures, the assignment of the 1674 cm^{-1} and the 1692 cm^{-1} bands can be narrowed down. After the investigation of the exponential amplitudes in Table 3, one can see that kinetics of the positive band at 1652 cm^{-1} and that of the negative ones at 1674 cm^{-1} and 1692 cm^{-1} are very similar. Therefore, they can be assigned to the same transition, i.e., most likely the new position of one of the 1674 cm^{-1} and 1692 cm^{-1} bands is the 1652 cm^{-1} band in the N state. Consequently, the possible candidates for the origin of these bands have to simultaneously satisfy the orientation conditions for the ground state (Θ_{1674} = 37 ± 2° or Θ_{1692} = 49 ± 2°) and for the N state (Θ_{1652} = 62 ± 7°). Ile-108 satisfies these conditions in both structures, Ala-143 and Trp-189, only in the model of Sass et al. (2000) having lower values for N state in Luecke et al. (1999) (42° and 50°, respectively) and Leu-92 in the model of Luecke et al. (1999) owing a much lower value in Sass et al. (2000) (15°) (Fig. 7 *b*). Therefore, the best matches are Ile-108 and Trp-189. Ile-108 is at the cytoplasmic end of helix D, far from Asp-96 and the proposed proton transfer chain from Asp-96 to the Schiff base. Therefore, it possibly does not have any significant role in the function of bR. On the other hand, the rings of Trp-189 situating between Glu-194, member of the proton-release complex, and the retinal has been shown to undergo a directional change between bR and N even in the D96N mutant beside the wild type. We therefore propose that the 1692 cm^{-1} negative band shifts to the 1652 cm^{-1} positive band and tentatively assign them to a single group that is either Ile-108 or Trp-189.

The 1667 cm^{-1} band

The amplitude of the Gaussian curve fitted to the 1667 cm^{-1} band is negative for the A_{II} spectrum series but it is positive for $A_{\perp}$. This behavior is strange if we consider the calculation of the angle Θ, which requires from A_{II} and $A_{\perp}$ to have identical sign. It can be explained if we assume that the dipole moment of the C═O group, which vibrates with this frequency in the bR state, simply changes its orientation during the bR→M transition without changing its frequency. This also explains why this band is not seen in the M state in nonpolarized measurements and why it appears in polarized photoselection measurements when the parallel and perpendicular directions are measured separately (Breton and Nabedryk, 1989).

This argument is supported by kinetic calculations (Fig. 8), too. First, the amplitude of the Gaussian of this band is positive for the perpendicular polarization, and it is negative for the parallel one at the very first time slice (~78 ms after the laser flash). At this time almost exclusively the M state is present, as seen from the difference spectra. This means that in the M state, the parallel component of the absorption of this band is smaller, and the perpendicular is larger relative to that in the bR state. So in the M intermediate its frequency is the same as in bR but its orientation is not.

In the next step we fitted exponentials to the Gaussian amplitudes of the amide bands and found that the exponential amplitudes of the first time constant ($a_{1,II}$ and $a_{1,\perp}$ of τ_1 = 0.44 s) of this band have the same positive sign, but those of the second one (τ_2 = 2.42 s) are opposite: $a_{2,II}$ is negative and $a_{2,\perp}$ is positive. $a_{3,II}$ and $a_{3,\perp}$ for the 1667 cm^{-1} band have also the same sign: they are both negative. The positiveness of both a_1 amplitudes means that both the parallel and perpendicular Gaussian amplitudes decrease with the

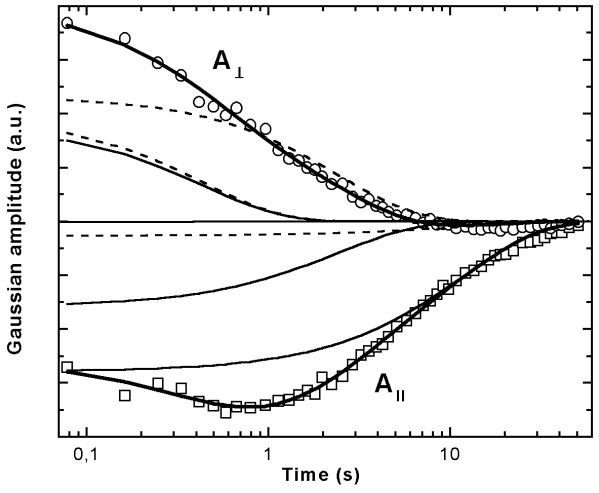

FIGURE 8 The Gaussian amplitude of the 1667 cm^{-1} band measured in parallel (□) and perpendicular (○) polarized IR light in respect to that of the actinic light. The time dependent amplitudes were fitted to a sum of exponentials (*thick line*). The individual exponential components were also calculated both in the parallel (*thin line*) and in the perpendicular (*dashed line*) cases.

first time constant. This is consistent with what we found earlier, namely, that the $\tau_1 = 0.44$-s time constant represents the M→N decay. In this frame we can explain the decrease of the Gaussian amplitude of the 1667 cm^{-1} band with $\tau_1 =$ 0.44 s in the parallel (A_{II}) case to a more negative value and its concurrent decrease in the perpendicular ($A_{\perp}$) case toward zero. These decreases show that the frequency of the dipole shifts from its original value in both the bR and M states to a new value in N. The new frequency of the dipole in the N state is not known, however. We can summarize that with $\tau_1 = 0.44$ s not only the M state decays but the N builds up, which is shown by the appearance of the negative 1667 cm^{-1} band.

The question, why the positive perpendicular Gaussian amplitude of the 1667 cm^{-1} band does not become negative as well can probably be answered with the recovery of the bR state.

CONCLUSIONS

By performing polarized time resolved FTIR experiments we were able to characterize motions of the carboxylic groups, the Schiff base, and some amide I dipoles during the photocycle. Comparison of recent x-ray diffraction data with FTIR spectroscopy results helped the assignment of bands in the infrared spectra that have been intensively studied earlier in spectroscopy studies. In addition, the comparison of the data made the identification of the protonated oxygen in carboxylic groups possible. As new x-ray structure results emerge, such comparative studies should be further pursued. Time-resolved spectroscopy (both infrared and visible) yields highly detailed dynamic information about the photocycle reactions, whereas the more static x-ray structures has atomic resolution: the combination of the two approaches may result in a complete understanding of the events during function.

The authors acknowledge fruitful discussions with A. Dér, G. Groma, and G. Váró.

This work was supported by grant Országos Tudományos Kutatási Alap No. T29764.

REFERENCES

Bagley, K., G. Dollinger, L. Eisenstein, A. K. Singh, and L. Zimányi. 1982. Fourier transform infrared difference spectroscopy of bacteriorhodopsin and its photoproducts. *Proc. Natl. Acad. Sci. U.S.A.* 79:4972–4976.

Barabás, K., A. Dér, Zs. Dancsházy, P. Ormos, L. Keszthelyi, and M. Marden. 1983. Electro-optical measurements on aqueous suspension of purple membrane from *Halobacterium Halobium. Biophys. J.* 43:5–11.

Becher, B., and T. G. Ebrey. 1977. The quantum efficiency for the photochemical conversion of the purple membrane protein. *Biophys. J.* 17:185–191.

Belrhali, H., P. Nollert, A. Royant, C. Menzel, J. P. Rosenbusch, E. M. Landau, and E. Pebay-Peyroula. 1999. Protein, lipid and water organization in bacteriorhodopsin crystals: a molecular view of the purple membrane at 1.9 Å resolution. *Structure.* 7:909–917.

Breton, J., and E. Nabedryk. 1989. Light-induced polarized Fourier transform infrared spectroscopy of bacteriorhodopsin: a study of the M_{412} intermediate by photoselection. *Biochim. Biophys. Acta.* 973:13–18.

Czégé, J., A. Dér, L. Zimányi, and L. Keszthelyi. 1982. Restriction of motion of protein side chains during the photocycle of bacteriorhodopsin. *Proc. Natl. Acad. Sci. U.S.A.* 79:7273–7277.

Earnest, T. N., P. Roepe, M. S. Braiman, J. Gillespie, and K. J. Rothschild. 1986. Orientation of the bacteriorhodopsin chromophore probed by polarized Fourier transform infrared difference spectroscopy. *Biochemistry.* 25:7793–7798.

Fahmy, K., F. Siebert, M. F. Groβjean, and P. Tavan. 1989. Photoisomerization in bacteriorhodopsin studied by FTIR, linear dichroism and photoselection experiments combined with quantum chemical theoretical analysis. *J. Mol. Struct.* 214:257–288.

Fahmy, K., F. Siebert, and P. Tavan. 1991. Structural investigation of bacteriorhodopsin and some of its photoproducts by polarized Fourier transform infrared spectroscopic methods-difference spectroscopy and photoselection. *Biophys. J.* 60:989–1001.

Gerwert, K., G. Souvignier, and B. Hess. 1990. Simultaneous monitoring of light-induced changes in protein side-group protonation, chromophore isomerization, and backbone motion of bacteriorhodopsin by time-resolved Fourier-transform infrared spectroscopy. *Proc. Natl. Acad. Sci. U.S.A.* 87:9774–9778.

Goldschmidt, C. R., O. Kalisky, T. Rosenfeld, and M. Ottolenghi. 1977. The quantum efficiency of the bacteriorhodopsin photocycle. *Biophys. J.* 17:179–183.

Hatanaka, M., H. Kandori, and A. Maeda. 1997. Localization and orientation of functional water molecules in bacteriorhodopsin as revealed by polarized Fourier transform infrared spectroscopy. *Biophys. J.* 73: 1001–1006.

Heberle, J. 2000. Proton transfer reactions across bacteriorhodopsin and along the membrane. *Biochim. Biophys. Acta.* 1458:135–147.

Heyn, M. P., and H. Otto. 1992. Photoselection and transient linear dichroism with oriented immobilized purple membranes: evidence for motions of the C(20)-methyl group of the chromophore towards the cytoplasmic side of the membrane. *Photochem. Photobiol.* 56: 1105–1112.

Kandori, H. 1998. Polarized FTIR spectroscopy distinguishes peptide backbone changes in the M and N photointermediates of bacteriorhodopsin. *J. Am. Chem. Soc.* 120:4546–4547.

Ludmann, K., Cs. Gergely, A. Dér, and Gy. Váró. 1998. Electric signals during the bacteriorhodopsin photocycle, determined over a wide pH range. *Biophys. J.* 75:3120–3126.

Luecke, H., B. Schobert, J.-P. Cartailler, H.-T. Richter, A. Rosengarth, R. Needleman, and J. K. Lanyi. 2000. Coupling photoisomerization of retinal to directional transport in bacteriorhodopsin. *J. Mol. Biol.* 300: 1237–1255.

Luecke, H., B. Schobert, H.-T. Richter, J.-P. Cartailler, and J. K. Lanyi. 1999. Structural changes in bacteriorhodopsin during ion transport at 2 Angstrom resolution. *Science.* 286:255–260.

Marsh, D., M. Müller, and F.-J. Schmitt. 2000. Orientation of the infrared transition moments for an α-helix. *Biophys. J.* 78:2499–2510.

Nabedryk, E., and J. Breton. 1986. Polarized Fourier transform infrared (FTIR) difference spectroscopy of the M_{412} intermediate in the bacteriorhodopsin photocycle. *FEBS Lett.* 202:356–360.

Oesterhelt, D., and W. Stoeckenius. 1974. Isolation of the cell membrane of *Halobacterium halobium* and its fractionation into red and purple membrane. *Methods Enzymol.* 31:667–668.

Ormos, P. 1991. Infrared spectroscopic demonstration of a conformational change in bacteriorhodopsin involved in proton pumping. *Proc. Natl. Acad. Sci. U.S.A.* 88:473–477.

Ormos, P., K. Chu, and J. Mourant. 1992. Infrared study of the L, M, and N intermediates of bacteriorhodopsin using the photoreaction of M. *Biochemistry.* 31:6933–6937.

Pfefferlé, J.-M., A. Maeda, J. Sasaki, and T. Yoshizawa. 1991. Fourier transform infrared study of the N intermediate of bacteriorhodopsin. *Biochemistry.* 30:6548–6556.

Rammelsberg, R., G. Huhn, M. Lübben, and K. Gerwert. 1998. Bacteriorhodopsin's intramolecular proton-release pathway consists of a hydrogen-bonded network. *Biochemistry.* 37:5001–5009.

Rothschild, K. J., and N. A. Clark. 1979. Polarized infrared spectroscopy of oriented purple membrane. *Biophys. J.* 25:473–488.

Rothschild, K. J., T. Marti, S. Sonar, Y.-W. He, P. Rath, W. Fischer, and H. G. Khorana. 1993. Asp96 deprotonation and transmembrane α-helical structural changes in bacteriorhodopsin. *J. Biol. Chem.* 268: 27046–27052.

Sasaki, J., J. K. Lanyi, R. Needleman, T. Yoshizawa, and A. Maeda. 1994. Complete identification of C = O stretching vibrational bands of protonated aspartic acid residues in the difference infrared spectra of M and N intermediates versus bacteriorhodopsin. *Biochemistry.* 33:3178–3184.

Sasaki, J., Y. Shichida, J. K. Lanyi, and A. Maeda. 1992. Protein changes associated with reprotonation of the Schiff-base in the photocycle of Asp96→Asn bacteriorhodopsin. *J. Biol. Chem.* 267:20782–20786.

Sass, H. J., G. Büldt, R. Gessenich, D. Hehn, D. Neff, R. Schlesinger, J. Berendzen, and P. Ormos. 2000. Structural alterations for proton translocation in the M state of wild-type bacteriorhodopsin. *Nature.* 406: 649–652.

Smith, S. O., A. B. Myers, R. A. Mathies, J. A. Pardoen, C. Winkel, E. M. M. van den Berg, and J. Lugtenburg. 1985. Vibrational analysis of the all-*trans* retinal protonated Schiff-base. *Biophys. J.* 47:653–664.

Váró, Gy. and J. K. Lányi. 1991. Thermodynamics and energy coupling in the bacteriorhodopsin photocycle. *Biochemistry.* 30:5016–5022.

Weidlich, O., and F. Siebert. 1993. Time-resolved step-scan FT-IR investigations of the transition from KL to L in the bacteriorhodopsin photocycle: identification of chromophore twists by assigning hydrogen-out-of-plane (HOOP) bending vibrations. *Appl. Spectr.* 47:1394–1400.

Yamazaki, Y., H. Kandori, R. Needleman, J. K. Lanyi, and A. Maeda. 1998. Interaction of the protonated Schiff-base with the peptide backbone of Valine 49 and the intervening water molecule in the N photointermediate of bacteriorhodopsin. *Biochemistry.* 37:1559–1564.